

ignoring the mass contribution of hydrogen.

The abundances and depletions of the elements provide a searching test for the proposal (§1.4) that biota are ubiquitous in the interstellar medium. The biological model for interstellar grains would require a higher degree of C depletion than is generally observed, in common with other grain models, and does not readily account for the high depletions of the metals. A more critical objection concerns the element phosphorus (Duley 1984; Whittet 1984a). Phosphates are an integral part of nucleic acid chains, and the numerical abundance of P in bacteria relative to that of C is typically $[N(P)/N(C)]_B \simeq 0.02$. Assuming solar abundances for the ISM and allowing for the observational result that the depletion of P typically exceeds that of C by a factor ~ 2 , the ratio in interstellar dust is $[N(P)/N(C)]_d \simeq 0.002$. Thus, no more than $\sim 10\%$ of the depleted C, or $\sim 2\%$ of the total grain density, can be in bacterial grains. Similar arguments apply to viruses. If biota were widespread in molecular clouds and desiccated in the lower-density clouds and intercloud gas available to depletion analysis, then desorption should lead to gas phase abundances of P significantly *enhanced* over the solar value, contrary to observations.

3

Interstellar Extinction and Scattering

"Further, there is the importance of getting an insight into the true spectrum of the stars, freed from the changes brought about by the medium traversed by light on its way to the observer."

J C Kapteyn (1909)

Extinction occurs whenever electromagnetic radiation is propagated through a medium containing small particles. In general, the transmitted beam is reduced in intensity by two physical processes, absorption and scattering. The energy of an absorbed photon is converted into internal energy of the particle, which is thus heated, whilst a scattered photon is deflected from the line of sight. The spectral dependence of continuum extinction, or extinction curve, is a function of the composition and size distribution of the particles. The polarization of starlight provides evidence that at least one component of the grains responsible for the extinction has anisotropic optical properties, most probably due to elongated shape and alignment by the galactic magnetic field, a topic discussed in detail in Chapter 4. In considering the extinction properties of the dust, spherical grains may be assumed in model calculations without loss of generality. In this chapter, we begin by outlining the theoretical basis for models of extinction and scattering. The relevant observations are then reviewed, considering, firstly, the average extinction curve for the interstellar medium within a few kiloparsecs of the Sun, and, secondly, departures from the average curve in lines of sight which sample different interstellar environments. The final section discusses attempts to match observations with theory.

3.1 THEORY AND METHODS

3.1.1 Extinction by Spheres

Suppose that spherical dust grains of radius a are distributed uniformly with number density n_d per unit volume along the line of sight to a distant star. The number of grains contained within a cylindrical column of length L and unit cross-sectional area is $N_d = n_d L$. Considering a discrete element of column with length dL , the fractional reduction in intensity of starlight at a given wavelength due to extinction within the element is

$$\frac{dI}{I} = -n_d C_{\text{ext}} dL \quad (3.1)$$

where C_{ext} is the extinction cross-section. Integrating equation (3.1) over the entire path-length gives

$$I = I_0 e^{-\tau} \quad (3.2)$$

where I_0 is the initial value of I ($L = 0$), and

$$\begin{aligned} \tau &= n_d C_{\text{ext}} L \\ &= N_d C_{\text{ext}} \end{aligned} \quad (3.3)$$

is the optical depth of extinction due to dust. Expressing the intensity reduction in magnitudes, the total extinction at some wavelength λ is given by

$$\begin{aligned} A_\lambda &= -2.5 \log \left(\frac{I}{I_0} \right) \\ &= 1.086 N_d C_{\text{ext}} \end{aligned} \quad (3.4)$$

using equations (3.2) and (3.3). A_λ is more usually expressed in terms of the extinction efficiency factor Q_{ext} , given by the ratio of extinction cross-section to geometric cross-section:

$$Q_{\text{ext}} = \frac{C_{\text{ext}}}{\pi a^2} \quad (3.5)$$

Hence,

$$A_\lambda = 1.086 N_d \pi a^2 Q_{\text{ext}} \quad (3.6)$$

If, instead of grains of constant radius a , we have a size distribution such that $n(a) da$ is the number of grains per unit volume in the line of sight with radii in the range a to $a + da$, then equation (3.6) is replaced by

$$A_\lambda = 1.086 \pi \int a^2 Q_{\text{ext}}(a) n(a) da. \quad (3.7)$$

The problem of evaluating the expected spectral dependence of extinction A_λ for a given grain model (assumed composition and size distribution) is essentially that of evaluating Q_{ext} . The extinction efficiency is the sum of corresponding factors for absorption and scattering,

$$Q_{\text{ext}} = Q_{\text{abs}} + Q_{\text{sca}} \quad (3.8)$$

These efficiencies are functions of two quantities, a dimensionless size parameter,

$$x = \frac{2\pi a}{\lambda} \quad (3.9)$$

and a composition parameter, the complex refractive index of the grain material,

$$m = n - ik. \quad (3.10)$$

Q_{abs} and Q_{sca} may, in principle, be calculated for any assumed grain model, and the resulting values of total extinction compared with observational data. The problem is that of solving Maxwell's equations with appropriate boundary conditions at the grain surface. A solution was first formulated by Mie (1908) and independently by Debye (1909), resulting in what is now known as the Mie theory. A detailed treatment of Mie theory is beyond the scope of this book; excellent modern accounts of both the theory and its applications are available in the literature (van de Hulst 1957; Bohren and Huffman 1983), to which the reader is referred for further discussion.

In order to compute the extinction curve for an assumed grain composition, the real and imaginary parts of the refractive index (equation (3.10)) must be specified. These quantities, n and k , somewhat misleadingly called the 'optical constants', are, in general, functions of wavelength. For dielectric materials ($k = 0$) the refractive index is given empirically by the Cauchy formula

$$m = n \simeq c_1 + c_2 \lambda^{-2} \quad (3.11)$$

where c_1 and c_2 are the Cauchy constants. In general, $c_1 \gg c_2$ and so n is only weakly dependent on λ for dielectrics. Ices and silicates are examples of astrophysically significant solids which behave as good dielectrics ($k \leq 0.05$) over much of the electromagnetic spectrum. For strongly absorbing materials such as metals, k is of the same order as n and both may vary strongly with wavelength.

Figure 1.1 shows sample plots of Q_{ext} and Q_{sca} versus x for constant refractive indices $1.6 - 0.0i$ and $1.6 - 0.05i$. In the former case, the particles are purely dielectric, and $Q_{\text{ext}} = Q_{\text{sca}}$ ($Q_{\text{abs}} = 0$); in the latter, the particles are slightly absorbing and $Q_{\text{ext}} > Q_{\text{sca}}$. For constant particle radius a , the Q_{ext} plots of are equivalent to extinction curves expressed as A_λ ($\propto Q_{\text{ext}}$) versus λ^{-1} ($\propto x$). For $x < 3$ ($\lambda > 2a$), extinction increases steadily with λ in both plots, and a region occurs near $x = 1.7$ where $Q_{\text{ext}} \propto x$ ($A_\lambda \propto \lambda^{-1}$) to a good approximation. At larger values of x , resonances occur in the extinction curves for single grain radii which are smoothed out when the contributions of grains with many different radii in a size distribution are summed (equation (3.7)). At very large values of x ($a \gg \lambda$), Q_{ext} is constant, and we have neutral extinction.

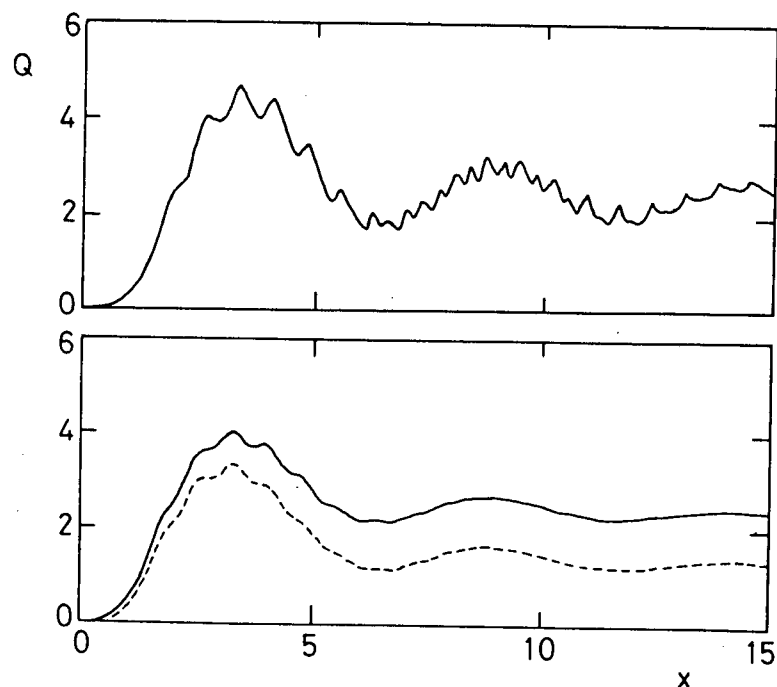


Figure 3.1 Plots of efficiency factors Q_{ext} and Q_{sca} against x for spherical grains. Upper frame: $m = 1.6 - 0.0i$; $Q_{\text{ext}} = Q_{\text{sca}}$. Lower frame: $m = 1.6 - 0.05i$; solid curve is Q_{ext} , dashed curve is Q_{sca} .

When $x \ll 1$ (i.e., the particles are small compared with the wave-

length), useful approximations may be used to give simple expressions for the efficiency factors (see Bohren and Huffman 1983, ch. 5):

$$Q_{\text{sca}} \approx \frac{8}{3} x^4 \left| \frac{m^2 - 1}{m^2 + 2} \right|^2 \quad (3.12)$$

and

$$Q_{\text{abs}} \approx 4x \Im \left\{ \frac{m^2 - 1}{m^2 + 2} \right\}. \quad (3.13)$$

For pure dielectric spheres, m is real and nearly constant, as discussed above, and thus $Q_{\text{ext}} = Q_{\text{sca}} \propto x^4 \propto \lambda^{-4}$ in the small-particle approximation (Rayleigh scattering). More generally, the quantity $(m^2 - 1)/(m^2 + 2)$ is often only weakly dependent on wavelength for materials which are not strongly absorbing, in which case $Q_{\text{abs}} \propto \lambda^{-1}$ to a good approximation, whilst $Q_{\text{sca}} \propto \lambda^{-4}$, as before. In this case, extinction dominated by absorption in the small-particle limit gives a λ^{-1} dependence, whilst extinction dominated by scattering gives a λ^{-4} dependence.

3.1.2 Albedo, Scattering Function and Asymmetry Parameter

Further quantities of interest, describing the scattering properties of the grains, may be deduced from the Mie theory. The albedo is defined by

$$\gamma = \frac{Q_{\text{sca}}}{Q_{\text{ext}}} \quad (3.14)$$

and is hence specified as a function of wavelength for a given grain model. As $Q_{\text{ext}} \geq Q_{\text{sca}} \geq 0$, we have $0 \leq \gamma \leq 1$. For pure dielectrics ($k = 0$), $Q_{\text{ext}} = Q_{\text{sca}}$ and hence $\gamma = 1$. For strong absorbers ($k \sim n$), $Q_{\text{sca}} \approx 0$ and thus $\gamma \approx 0$. Thus, observational measurements of γ may be used to place constraints on the imaginary (absorptive) component of the refractive index.

The scattering function $S(\theta)$ describes the angular redistribution of light upon scattering by a dust grain. It is defined such that, for light of incident intensity I_0 , the intensity of light scattered into unit solid angle about the direction at angle θ to the direction of propagation of the incident beam is $I_0 S(\theta)$ (assuming axial symmetry). The scattering cross-section, defined as $C_{\text{sca}} = \pi a^2 Q_{\text{sca}}$ by analogy with equation (3.5), is related to $S(\theta)$ by

$$C_{\text{sca}} = 2\pi \int_0^\pi S(\theta) \sin \theta d\theta. \quad (3.15)$$

The asymmetry parameter is defined as the mean value of $\cos \theta$ weighted with respect to $S(\theta)$:

$$\begin{aligned} g(\theta) &= \langle \cos \theta \rangle \\ &= \frac{\int_0^\pi S(\theta) \sin \theta \cos \theta \, d\theta}{\int_0^\pi S(\theta) \sin \theta \, d\theta} \\ &= \frac{2\pi}{C_{\text{sca}}} \int_0^\pi S(\theta) \sin \theta \cos \theta \, d\theta. \end{aligned} \quad (3.16)$$

Calculations for dielectric spheres show that $g(\theta) \simeq 0$ in the small-particle limit, which corresponds to spherically symmetric scattering, whereas $0 < g(\theta) < 1$ for larger particles, indicating forward-directed scattering. As the ratio of grain diameter to wavelength increases from 0.3 to 1.0, a range of particular interest for studies of interstellar dust, the value of $g(\theta)$ increases from 0.15 to 0.75. Hence, the asymmetry parameter is a sensitive function of grain size (Witt 1989).

3.1.3 The Colour-Difference Technique

Consider two stars of identical spectral type and luminosity class but unequal reddening. The apparent magnitude of each star as a function of wavelength is given by

$$m_1(\lambda) = M_1(\lambda) + 5 \log d_1 + A_1(\lambda)$$

and

$$m_2(\lambda) = M_2(\lambda) + 5 \log d_2 + A_2(\lambda) \quad (3.17)$$

where M represents absolute magnitude, d distance, and A the total extinction (see §1.1.1). The intrinsic spectral energy distribution is expected to be the same for stars of the same spectral classification; thus $M_1(\lambda) = M_2(\lambda)$. If we also assume that $A(\lambda) = A_1(\lambda) \gg A_2(\lambda)$, i.e. the extinction towards star 2 is negligible compared with that towards star 1, then the magnitude difference $\Delta m(\lambda) = m_1(\lambda) - m_2(\lambda)$ reduces to

$$\Delta m(\lambda) = 5 \log \left(\frac{d_1}{d_2} \right) + A(\lambda). \quad (3.18)$$

The first term on the RHS of equation (3.18) is independent of wavelength and constant for a given pair of stars. Hence, the quantity $\Delta m(\lambda)$ may be used to represent $A(\lambda)$. This technique is termed the 'colour-difference' or 'pair' method.

The interstellar extinction curve has traditionally been studied by the colour-difference method using low-resolution spectrophotometry, broadband photometry, or some combination of these. When spectrophotometry

of resolution $\Delta\lambda < 50 \text{ \AA}$ is used, matching of individual stellar spectral lines in the reddened and comparison stars becomes important. Early-type stars (spectral classes O–A0) are generally selected for such investigations as their spectra are relatively simple and thus easy to match, and their intrinsic luminosity and frequent spatial association with dusty regions also render them most suitable for probing the interstellar medium at optical and ultraviolet wavelengths. As an example of the application of the colour-difference method, figure 2.2 plots the observed spectra in the visible (4000–6500 \AA) for a matching pair of stars, and the resulting extinction curve. The stars selected are ζ Oph (spectral type O9.5V, reddening $E_{B-V} = 0.32$) and ν Ori (B0V, $E_{B-V} = 0.03$). Flux density ($\log F_\lambda$) and extinction, Δm (equation (3.18)) are plotted against wavenumber λ^{-1} . Note the cancellation of stellar spectral lines to produce a smooth extinction curve.

The constant term in equation (3.18) may be eliminated by means of normalization with respect to two standard wavelengths λ_1 and λ_2 :

$$\begin{aligned} E_{\text{norm}} &= \frac{\Delta m(\lambda) - \Delta m(\lambda_2)}{\Delta m(\lambda_1) - \Delta m(\lambda_2)} \\ &= \frac{A(\lambda) - A(\lambda_2)}{A(\lambda_1) - A(\lambda_2)} \\ &= \frac{E(\lambda - \lambda_2)}{E(\lambda_1 - \lambda_2)}. \end{aligned} \quad (3.19)$$

The normalized extinction E_{norm} should be independent of stellar parameters and determined purely by the extinction properties of the interstellar medium. Normalized curves for different stars may be superposed and compared. Theoretical extinction curves deduced from equation (3.7) for a given grain model may also be normalized in the same way to allow direct comparison between observations and theory. When broadband photometry tied to a standard photometric system is used, it is not essential to observe unreddened comparison stars, as the reddened stars may be compared with tabulated intrinsic colours (e.g. Johnson 1966). Extinction curves are commonly normalized with respect to the B and V passbands in the Johnson system.

Two difficulties associated with the colour-difference method should be noted. Firstly, there is a scarcity of suitable comparison stars for detailed spectrophotometry, as relatively few OB stars are close enough to the Sun or at high enough galactic latitude to have negligible reddening. The problem is most acute for supergiants, and these are often excluded from studies of extinction in the ultraviolet where mismatches in spectral line strengths can be particularly troublesome. Secondly, many early-type stars have infrared excess emission, due to thermal re-radiation from circumstellar dust or free-free emission from ionized gas, and if one attempts to derive the extinction curve for such an object by comparing it with a normal star

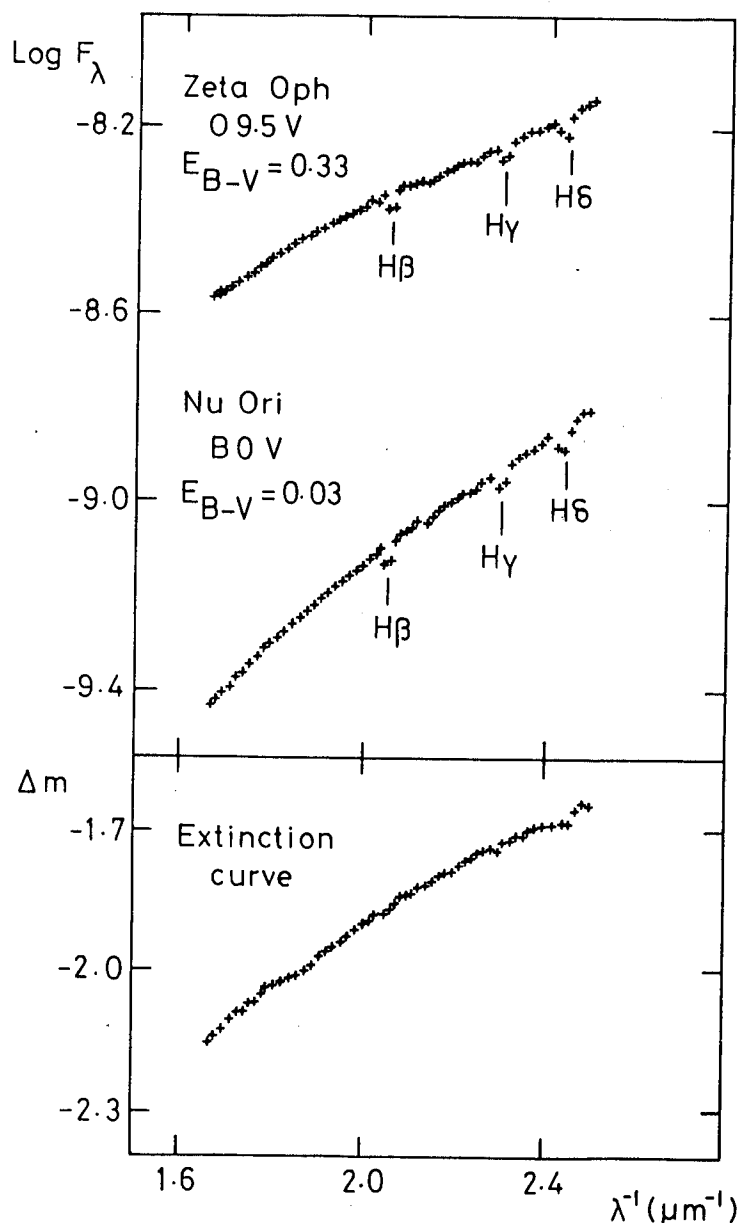


Figure 3.2 An illustration of the colour-difference method. Upper frame: plot of $\log F_\lambda$ ($\text{W m}^{-2} \mu\text{m}^{-1}$) against λ^{-1} (μm^{-1}) for the reddened star ζ Oph and the intrinsically similar unreddened star ν Ori (data from Willstrop 1965). Stellar spectral lines in the Balmer series are labelled. Lower frame: the resulting interstellar extinction curve for the dust towards ζ Oph.

or with normal intrinsic colours, the derived extinction curve will be distorted in the spectral bands at which significant emission occurs. If, for example, there is emission in the K -band at $2.2 \mu\text{m}$, then the colour excess ratio E_{V-K}/E_{B-V} is anomalously large (because K is numerically too small compared with V). This can lead to systematic overestimates of the ratio of total to selective extinction (§3.2.4). Fortunately, shell stars can usually be identified spectroscopically by the presence of optical emission lines, providing a means of discrimination (Whittet and van Breda 1978).

3.2 AVERAGE PROPERTIES

3.2.1 The Mean Extinction Curve

Reliable data on the wavelength dependence of extinction are available in the spectral region from 0.1 to $5 \mu\text{m}$. Studies of large samples of stars have shown that the extinction curve takes the same general form in many lines of sight. Regional variations are apparent, particularly in the blue-ultraviolet region of the spectrum, which we discuss in §3.3 below, but the average extinction curve for many stars provides a valuable benchmark for comparison with curves deduced for individual stars and regions, and a basis for modelling. The best available data, plotted in figure 3.3 and listed in table 3.1, are taken from the compilations of Whittet (1988) for the infrared ($1\text{--}5 \mu\text{m}$) and Savage and Mathis (1979) for the optical and ultraviolet ($0.1\text{--}1 \mu\text{m}$)†. The stars in the sample are reddened predominantly by diffuse clouds within $2\text{--}3$ kpc of the Sun.

The values of extinction presented in table 3.1 make use of standard normalizations. The relative extinction (replacing the labels λ_1 and λ_2 in equation (3.19) with B and V) is

$$\begin{aligned} \frac{E_{\lambda-V}}{E_{B-V}} &= \frac{A_\lambda - A_V}{E_{B-V}} \\ &= R_V \left\{ \frac{A_\lambda}{A_V} - 1 \right\}. \end{aligned} \quad (3.20)$$

Thus, the *absolute* extinction A_λ/A_V may be deduced from the relative extinction if $R_V = A_V/E_{B-V}$, the ratio of total to selective extinction, is known. The values of A_λ/A_V in table 3.1 are deduced for a value of $R_V = 3.05$ (see §3.2.4 below).

† A correction has been applied to remove a spurious bump near $6.3 \mu\text{m}^{-1}$, which arose due to mismatched stellar CIV lines (Massa *et al* 1983) in part of the data set used by Savage and Mathis.

THE GRADUATE

SERIES IN

ASTRONOMY

Series Editors

R. J. Kolar

R. E. Witt

DUST IN THE GALACTIC ENVIRONMENT

DCB Whittet

